



# Environmentally friendly packaging foams: Investigation of the compostability of poly(lactic acid)-based syntactic foams

Katalin Litauszki<sup>a</sup>, Dániel Gere<sup>a,b</sup>, Tibor Czigany<sup>a,c</sup>, Ákos Kmetty<sup>a,c,\*</sup>

<sup>a</sup> Department of Polymer Engineering, Faculty of Mechanical Engineering, Budapest University of Technology and Economics, Műegyetem rkp. 3, H-1111 Budapest, Hungary

<sup>b</sup> Imsys Ltd, Material Testing Laboratory, Mozaik Street 14/A., H-1033 Budapest, Hungary

<sup>c</sup> ELKH-BME Research Group for Composite Science and Technology, Műegyetem rkp. 3., H-1111 Budapest, Hungary

## ARTICLE INFO

### Keywords:

Foams  
Extrusion  
Environmental degradation  
Porosity

## ABSTRACT

We investigated how the compostability of polymeric foam samples is influenced by the D-lactide content of poly(lactic acid) and the presence and dosage of an expandable microspheres-type foaming agent. Our results show that the poly(lactic acid)-based foam sheet with higher D-lactide content decomposed faster (49 days) than the foam sheet with lower D-lactide content (63 days), when 8 wt% foaming agent was applied. As the degradation time is shorter for amorphous PLA due to the water diffusion through amorphous PLA. Furthermore, we found that in a poly(lactic acid)-based syntactic foam structures, thermally expandable microspheres decreased the rate of degradation, because not only matrix hydration should take place, but other mechanism like the hydration of the expandable microsphere and the polymer matrix interface as well. However, even the medium-density foams degraded before day 70.

## 1. Introduction

Today, plastics and products made from them (e.g., packaging) are used extensively. The total plastics production was 367 Mt. and the share of polymer materials used for packaging reached 40.5% of total plastic raw material consumption in 2020 [1]. The use of such plastic products (e.g., various packaging materials, foil and sheet products, foamed storage boxes) has been increased by the coronavirus pandemic (COVID-19) [2,3]. As the current consumption system is linear (take-make-waste perspective [4], such products with a short life cycle have a high environmental impact [5,6]. One possible solution to this problem is to implement a circular economy model [7]. A special type of polymer feedstock, biodegradable polymers, represents an important opportunity to contribute to a circular economy (biological cycles [8]). Biodegradable polymers are also, at best, annually renewable energy sources and biodegradable feedstocks [9–11]. Among the group of biodegradable polymers are polyhydroxyalkanoates (PHAs), poly(butylene adipate-co-terephthalate) (PBAT), polybutylene succinate (PBS), and poly(lactic acid) (PLA) [12–14]. PLA is one of the most important biopolymers because, among other things, it is economical to produce, can be processed with current polymer processing technologies, and can be

industrially composted [15] and recycled if necessary, i.e., it can be used to achieve circularity at both technological and biological levels [7]. Poly(lactic acid) is typically used in medical technology, pharmaceuticals, packaging, agriculture, and 3D printing [16–19]. Foaming of PLA is an important aspect and a promising possibility. Chemical and physical foaming of neat PLA has its limits, although modified PLA can be successfully foamed up to volume expansion ratio around 4 [20,21].

One of the very advantageous properties of poly(lactic acid) for the circular economy is that it can not only be produced from renewable resources (sugar cane, sugar beet, maize, potatoes, wheat) [22] but can also be biodegraded at elevated temperatures in a biotic environment [23]. The primary degradation mechanism of PLA is hydrolytic degradation, which occurs in two steps. First, random chain scrambling occurs at the ester groups, causing a loss of molecular weight. This phenomenon is accelerated by increased relative humidity, temperature, and pH [24,25]. Microorganisms are not yet involved in the primary degradation phase. As the average molecular weight decreases, microorganisms can digest the lower molecular weight lactide oligomers. The oligomers broken down by the microorganisms produce carbon dioxide and water. Degradation is accelerated in a compost media at elevated humidity and temperature (55–70 °C) [26]. The two-step degradation process of PLA

\* Corresponding author at: Department of Polymer Engineering, Faculty of Mechanical Engineering, Budapest University of Technology and Economics, Műegyetem rkp. 3, H-1111 Budapest, Hungary.

E-mail address: [kmetty@pt.bme.hu](mailto:kmetty@pt.bme.hu) (Á. Kmetty).

<https://doi.org/10.1016/j.susmat.2022.e00527>

Received 21 March 2022; Received in revised form 12 November 2022; Accepted 21 November 2022

Available online 26 November 2022

2214-9937/© 2022 The Authors. Published by Elsevier B.V. This is an open access article under the CC BY-NC-ND license (<http://creativecommons.org/licenses/by-nc-nd/4.0/>).

is an advantage over other single-step degradable biopolymers, as PLA is suitable for the proper storage of products and meets the regulatory requirements for food contact packaging [26]. One way to qualify for industrial compostability is composting under laboratory conditions. The ISO 20200:2015 standard provides a method for this. Gorrası and Pantani [27] investigated the effect of the morphology of PLA films (150  $\mu\text{m}$ ) on the first stage of the degradability process, i.e., hydrolytic degradation. For their work, they selected three types of PLA (Ingeo 4060D (12% D-lactide), 2002D (4% D-lactide), and 4032D (2% D-lactide)), which differ mainly in their D-lactide content, which greatly influences the crystallization kinetics and thus the morphology of the resulting polymer. They carried out degradability studies out at 58 °C. Ingeo 4060D PLA with the highest D-lactide content showed the fastest weight loss. Samples with lower D-lactide content (4% and 2%), amorphous or partially crystalline, showed similar but slower weight loss trends. The degradation process was also quantified by differential scanning calorimetry (DSC) and gel permeation chromatography (GPC). GPC confirmed chain rotation due to hydrolysis, whereby the molecular weight decreases over time. The DSC analysis (second heating curve) showed that the  $T_g$  of the samples decreased as the degradation process progressed. This phenomenon can be attributed to the increased molecular mobility caused by the chain shifting during hydrolysis. Sarasa et al. [28] investigated PLA-based products with different geometries. They sought to determine whether the product's geometry affected degradability and the rate of degradation. For this purpose, they produced various extruded and injection molded products, including chemically foamed PLA products. The degradability test was performed according to EN 14806 and ISO 20200:2004. Their results concluded that pores in foamed PLA might facilitate moisture exchange, thereby increasing biodegradation, which may promote microbial activity. Zimmermann et al. [29] also found similar results for poly(lactic acid) foamed with a chemical foaming agent. The foaming agent was a 2 wt% mixture of exothermic azodicarbonamide, endothermic sodium bicarbonate, and citric acid.

The research published so far has typically focused on the compostability of unfoamed poly(lactic acid) with thin or thick walls, with little information on the compostability of foamed biopolymers and no studies on the degradability of foam structures with expandable microspheres. Therefore, our research aimed to investigate the compostability of foam structures produced with the use of poly(lactic acid) as a feedstock. We chose a thermally expandable microsphere (EMS) foaming agent, and investigated the effect of the D-lactide content of poly(lactic acid) and the density of the foam structure, i.e., EMS content, on the degradability of the biopolymer-based foam structure.

## 2. Materials and methods

### 2.1. Materials

From the raw materials used for extrusion foaming, two types of poly(lactic acid) were selected. Ingeo™ 2003D (4.3% D-lactide content) semi-crystalline and 4060D (12.0% D-lactide content) amorphous PLA types manufactured by NatureWorks LLC (USA) [30]. The number average molecular weight of Ingeo 2003D was 100,422 g/mol, its weight average molecular weight was 180,477 g/mol, and its polydispersity index was 1.79. Ingeo 4060D had a number average molecular weight of 116,894 g/mol, a weight average molecular weight of 191,063 g/mol, and a polydispersity index of 1.63 [31]. The various PLA grades have a density of 1.24 g/cm<sup>3</sup> [32–35]. The expandable microsphere foaming agent used was Tracel G 6800 MS (Tramacı GmbH). The processing temperature of the PLA is decisive for the selection of the foaming agent, which ranges from 165 to 190 °C, with a recommended maximum processing temperature of 230 °C [36,37]. The shell structure of the expandable microspheres contains methyl methacrylate (16%), the polymeric carrier material is ethylene-vinyl acetate (36.8%) [31].

### 2.2. Preparation of specimens

Different samples of foamed material were prepared for the investigation of compostability parameters. From PLA with 12.0% D-lactide content, 0, 2, 4, and 8 wt% EMS foam sheets were prepared, and from PLA with 4.3% D-lactide content, 0 and 8 wt% EMS foam sheets were prepared. An example of sample nomenclature in the case of a 12.0% D-lactide PLA and 8 wt% EMS is the following: 12.0%PLA\_8wt%EMS. Before processing, the different PLA materials were dried in a Faithful WGLL-125 BE hot air oven at 80 °C for 6 h. The unfoamed and foamed sheets were manufactured on a flat film production line with a sheet production die. The material flow exiting the coat-hanger die was fed to a tempered roller with a polished surface driven by a pair of pneumatic rollers (Labtech Scientific 25-30C single screw extruder with LRC300 flat film line). The temperature profile was 155/160/175/190/190/190/190 °C. The coat-hanger die had an adjustable gap size set to the maximum, 4 mm. The width of the tool was 300 mm. The rotation speed of the screw was chosen to be 80 rpm to allow a sufficiently high pressure to build up in the die. The single screw was a conventional three-zone screw that has  $D = 25$  mm,  $L/D = 30$ . The temperature of the tempered, polished cylinder was chosen to be 40 °C, which is below the glass transition temperature of PLA, thus aiding the stabilization of the foam structure. The speed of the tempered, polished cylinder was 0.4 m/min, and pulling speed was 0.8 m/min, draw ratio was 2. No winding was used.

### 2.3. Testing methods

#### 2.3.1. Measurement of density

The density of the extruded samples was determined from the buoyant force according to Eq. (1) in distilled water at room temperature ( $23 \pm 2$  °C), where  $\rho$  [g/cm<sup>3</sup>] is sample density,  $m_{sa}$  [g] is the mass of the sample measured in air,  $m_{sl}$  [g] is the mass of the sample measured in distilled water and  $\rho_l$  [g/cm<sup>3</sup>] is the density of distilled water at the given temperature. The analytical balance used for measuring mass is an OHAUS Explorer, with a weighing capacity of 110 g and an accuracy of 0.1 mg.

$$\rho = \frac{m_{sa} \cdot \rho_l}{(m_{sa} - m_{sl})} \quad [\text{g}/\text{cm}^3] \quad (1)$$

Cell size and cell-population density was calculated based on the SEM images. Cell size was measured using ImageJ and defined as the diameter, at least 200 cells were measured. Cell-population density was calculated according to Eq. (2) [38], where  $n$  is the number of cells counted in the recorded image,  $A$  [cm<sup>2</sup>] is the cross-section area of the sample,  $M$  [–] is the magnification factor, and  $V_f$  [–] is the void fraction. The void fraction was calculated according to Eq. (3), where  $V_f$  [–] is the void fraction,  $\rho_{\text{foam}}$  is the density of the foamed polymer, and  $\rho_{\text{polymer}}$  is the density of the non-foamed polymer [38].

$$N_c = \left( \frac{n \cdot M^2}{A} \right)^{\frac{1}{3}} \cdot \frac{1}{1 - V_f} \quad (2)$$

$$V_f = 1 - \frac{\rho_{\text{foam}}}{\rho_{\text{polymer}}} \quad (3)$$

#### 2.3.2. Testing compostability

The compostability of PLA-based sheets was tested according to ISO 20200:2015 [39]. The composting medium was 40% sawdust, 30% alfalfa, 10% mature compost, 10% corn starch, 5% sucrose, 4% corn germ oil, 1% urea, and 55% distilled water with 45% dry matter content. Composting was carried out at 58 °C in a UT20 drying cabinet. The composting reactor was a 300 mm  $\times$  200 mm  $\times$  100 mm polypropylene box (with 5 mm diameter ventilation holes on both sides). The width and length of the test sheets were 25  $\times$  25 mm. The compost was mixed and the distilled water was replenished according to the standard.

According to ISO 20200:2015, a sample is considered degraded when residues pass through a 2 mm sieve. If pieces of the sample remain after sieving, the material is not considered degraded. In this case, the degradation rate can be calculated according to Eq. (4).

$$D = \frac{m_i - m_r}{m_i} [-] \quad (4)$$

where  $D$  [%] is the degree of disintegration,  $m_i$  [mg] is the initial mass of the test material, and  $m_r$  [mg] is the mass of the test material remaining after sieving [39].

### 2.3.3. Thermogravimetric analysis

The thermal decomposition characteristics of the foaming agents were investigated by thermogravimetric analysis. The thermogravimeter was a Q500 (TA Instruments, New Castle, DE, USA). The mass of the sample tested was 1–6 mg, the temperature range was 50–600 °C, and the heating rate was 10 °C/min. The measurement atmosphere and protecting gas of the balance was nitrogen. The volume flow rate of nitrogen was 40 ml/min (protective gas) and 60 ml/min (measurement atmosphere). Thermal decomposition was characterized with the initial degradation as the temperature corresponding to 5% weight reduction ( $T_{5\%}$  [°C]), the temperature corresponding to 50% weight reduction ( $T_{50\%}$  [°C]), and the temperature of the maximum of the weight change rate ( $T_{dT_{Gmax}}$  [°C]).

### 2.3.4. Differential scanning calorimetry

The DSC tests of the foam structures performed out with a TA Instruments Q2000 automatic sampler, with a heating-cooling-heating measurement program. The weight of the samples ranged from 3 to 6 mg. A heating-cooling-heating cycle was applied. The temperature range during the test was 0 to 200 °C. Both heating and cooling rates were 5 °C/min. The tests were performed in nitrogen gas with a 50 ml/min volume flow rate. The degree of crystallinity ( $\chi_c$ ) was calculated according to Eq. (5), where  $\Delta H_m$  is the enthalpy change during crystallization. The degree of crystallinity from production ( $\chi_{cf}$ ) was calculated according to Eq. (6), where  $\Delta H_m$  is the enthalpy change associated with crystalline melting and  $\Delta H_{cc}$  is the enthalpy change during cold crystallization.  $\alpha$  is the weight percent of EMS, PLA<sub>100%</sub> is the theoretical enthalpy of crystallization of 100% crystalline PLA, which is 93 J/g [40–42].

$$\chi_c = \frac{\Delta H_m}{\text{PLA}_{100\%}(1 - \alpha/100)} \cdot 100 [\%] \quad (5)$$

$$\chi_{cf} = \frac{\Delta H_m - |\Delta H_{cc}|}{\text{PLA}_{100\%}(1 - \alpha/100)} \cdot 100 [\%] \quad (6)$$

### 2.3.5. Optical, scanning electron microscopy and visual inspection

The changes on the surface of the samples and the appearance of possible microcracks were studied with a Keyence VHX-500 optical microscope, whereas the matrix and foamed structure of the reference samples was characterized with the use of scanning electron microscope (JEOL JSM-6380LA, Jeol Ltd., Japan with an acceleration voltage of 10 kV) images of the cryogenic fracture surface of the reference samples. The degradation process of the samples was recorded with a camera.

## 3. Results

Compostability is of paramount importance for biopolymers, and this is also true for biopolymer-based foam structures.

### 3.1. The effect of D-lactide content on the compostability of poly(lactic acid)-based foam structures

The effect of D-lactide content on the compostability of poly(lactic acid)-based foam structures was studied in PLA matrix materials that

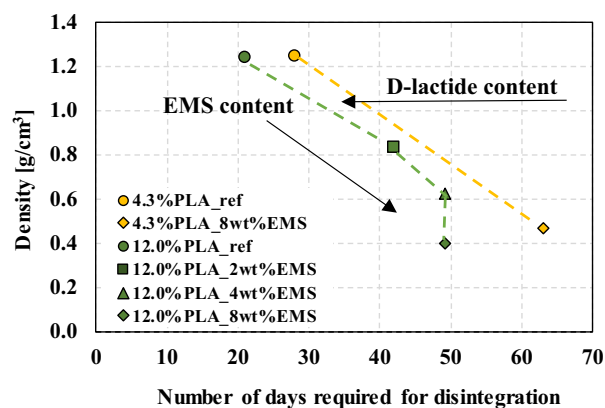


Fig. 1. Number of days required for sheet samples to degrade and sample density.

differ mainly in their D-lactide content [27,31]. The cell size distribution of the produced foams are homogeneous and because of the EMS foaming technique the cell-population density is increasing with higher foaming agent content (Supplementary A.1). During the composting study, the extent of decomposition was documented with photographs every 7 days, and DSC and TGA analysis were performed. The sample was considered to be degraded according to the standard when the size of the remaining fragments due to fragmentation is less than 2 mm. The number of days required for degradation is presented in Fig. 1, the density of the samples is according to Supplementary A.2. The degradation of the samples is shown in Fig. 2. During composting, the PLA matrix successfully decomposed in the case of PLA with 4.3% D-lactide content as well as in the case of PLA with 12.0% D-lactide content. The microsphere shell material (methyl methacrylate) is not degradable; therefore, it remains, which is still a problem at present. The polymeric carrier of the microsphere (ethylene-vinyl acetate) is also thought to remain, as it is present in the polymer matrix in the form of droplets of around 0.5–1.0 μm on scanning electron micrograph (Fig. 3 and in Supplementary A.3.). The droplet size in case of 12.0%PLA with 2wt% EMS is  $0.49 \pm 0.08 \mu\text{m}$ , with 4wt%EMS is  $0.74 \pm 0.24 \mu\text{m}$  and with 8wt%EMS is  $0.99 \pm 0.20 \mu\text{m}$ . The morphological properties of the samples were assessed by DSC and the degradation of the samples by TGA. Two types of PLA were investigated: Ingeo 2003D PLA (D-lactide content 4.3%), which tends to crystallize, and Ingeo 4060D PLA (D-lactide content 12.0%) with a tendency not to crystallize. The results show that the reference PLA sheet with higher D-lactide content (12.0%PLA\_ref) degraded faster, in 21 days, while the PLA sample with lower D-lactide content (4.3%PLA\_ref) degraded in 28 days. These results correlate with data in the literature, because D-lactide content has an effect on crystallization kinetics and crystallization kinetics greatly influences the morphology of the resulting polymer matrix. The difference between the number of days required for decomposition can be attributed to the crystalline fraction of PLA with 4.3% D-lactide content and PLA with 12.0% D-lactide content, because water diffusion through amorphous PLA results in higher hydrolysis in the polymer [43,44].

The extent of degradation was characterized by TGA (Fig. 4) and especially the temperature of initial degradation corresponding to 5% weight loss recorded during TGA (Fig. 5 a). Fig. 4 shows a general tendency. In the reference samples, the first TGA weight loss is related to the degradation of PLA. This weight loss step has a  $dT_{Gmax}$  temperature around 350 °C for both PLA with 4.3% and 12.0% D-lactide content. As a function of composting time, this first weight loss step shifts towards lower temperatures. Lower thermal stability indicates a PLA matrix with lower molecular weight [45]. The degradation of the polymer matrix, which was present in the highest proportion in the reference sample, was characterized by the temperature of the maximum of the derivative of mass loss (Fig. 5 b, Supplementary A.5). The faster degradation of PLA

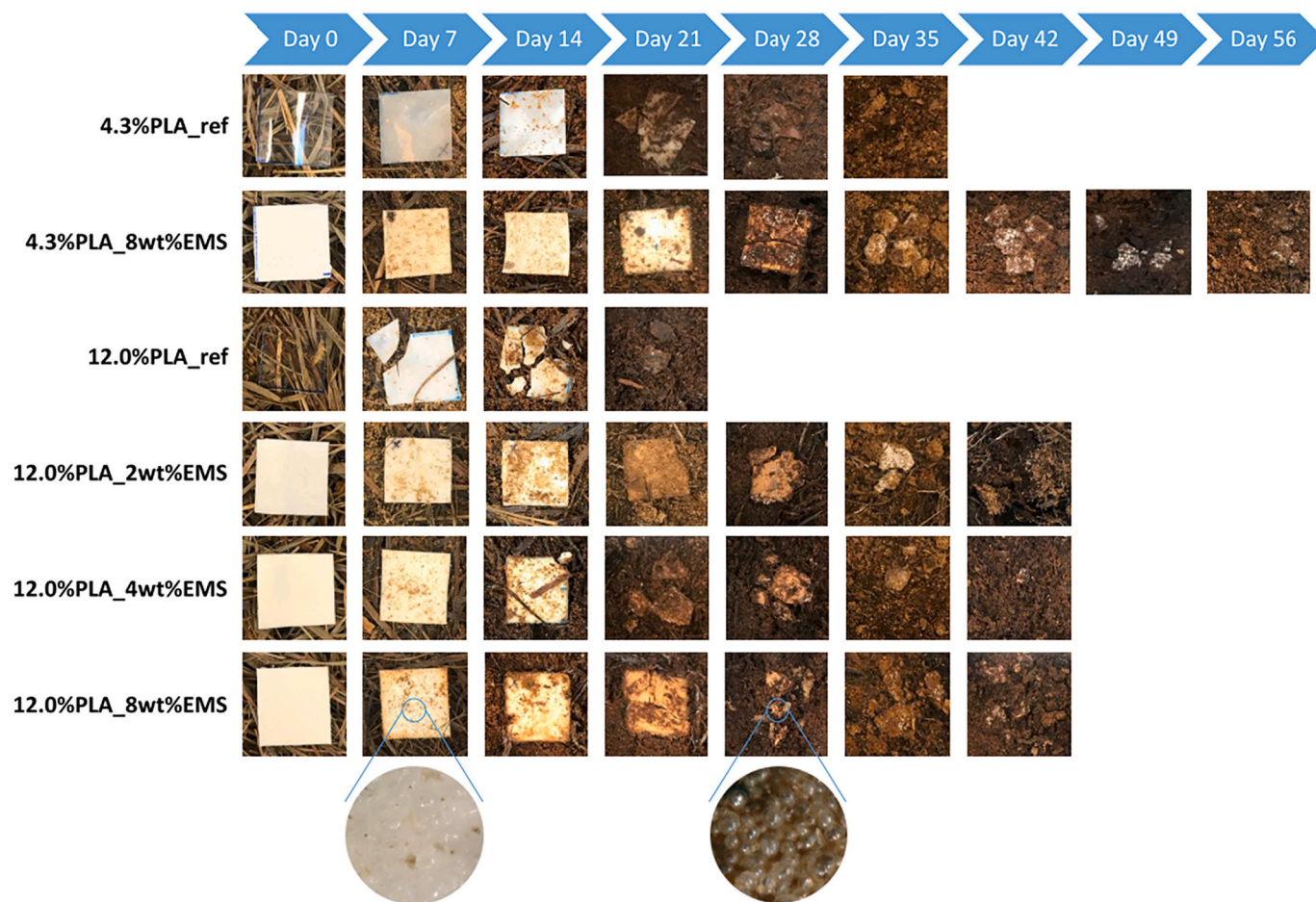


Fig. 2. Decomposition of sheet samples as a function of composting time.

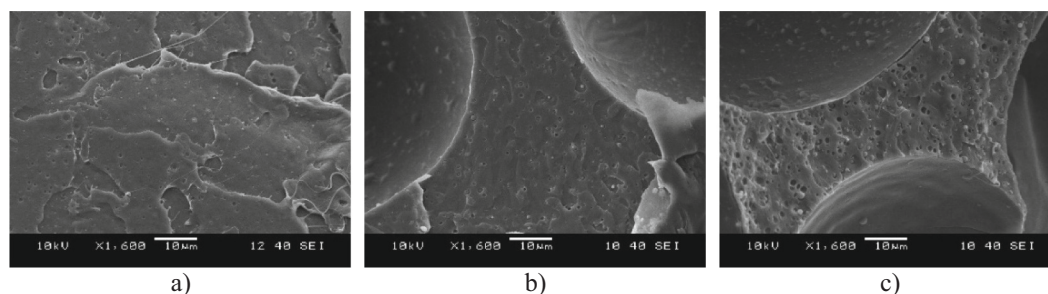


Fig. 3. SEM images of reference PLA (12.0% D-lactide) sheet samples containing a) 2 wt%, b) 4 wt%, c) 8 wt% expandable microsphere foaming agent (day 0).

with higher D-lactide content is shown by the rate of decrease of temperatures and  $T_{dT_{Gmax}}$  associated with  $T_{5\%}$ . The decrease in  $T_{5\%}$  and  $T_{dT_{Gmax}}$  can be explained with the fact that the polymer chains are broken by hydrolytic degradation during composting, and the length of the polymer chains is reduced. Lower temperatures are sufficient to decompose shorter polymer chains. However, the rate of hydrolysis also depends on the properties of PLA, such as crystallinity and initial molecular weight [46]. According to the literature, degradation time is shorter for low-molecular-weight, more hydrophilic and more amorphous polymers. At the initial stage of composting, the absorption of water molecules causes the ester bonds to randomly cleave, resulting in shortening of the polymer chains. When the molecular weight decreases to about 10,000 Da due to hydrolysis, the microorganisms start to degrade the PLA fragments. In addition, during composting, the

amorphous or less ordered parts are degraded first [44]. In the case of samples without a foaming agent, residual material content increases as a function of composting time. It is presumably a residue from the composting medium that cannot be removed completely from the sample before the measurement. Based on our results, Tracel G 6800 MS has a residual mass of 15.91% at 600 °C (Supplementary A.4), so for samples containing the foaming agent, these two residual masses add up to give the total residual mass.

The morphological properties of the extruded foam samples were investigated by DSC (Supplementary A.6). Sheet reference samples produced from PLA with 4.3% and 12.0% D-lactide contents were amorphous right after foaming (day 0). However, PLA samples with 4.3% D-lactide content cold crystallized during the DSC test. Cold crystallization enthalpy for 4.3%PLA\_ref was 26.1 J/g and for 4.3%PLA\_8wt

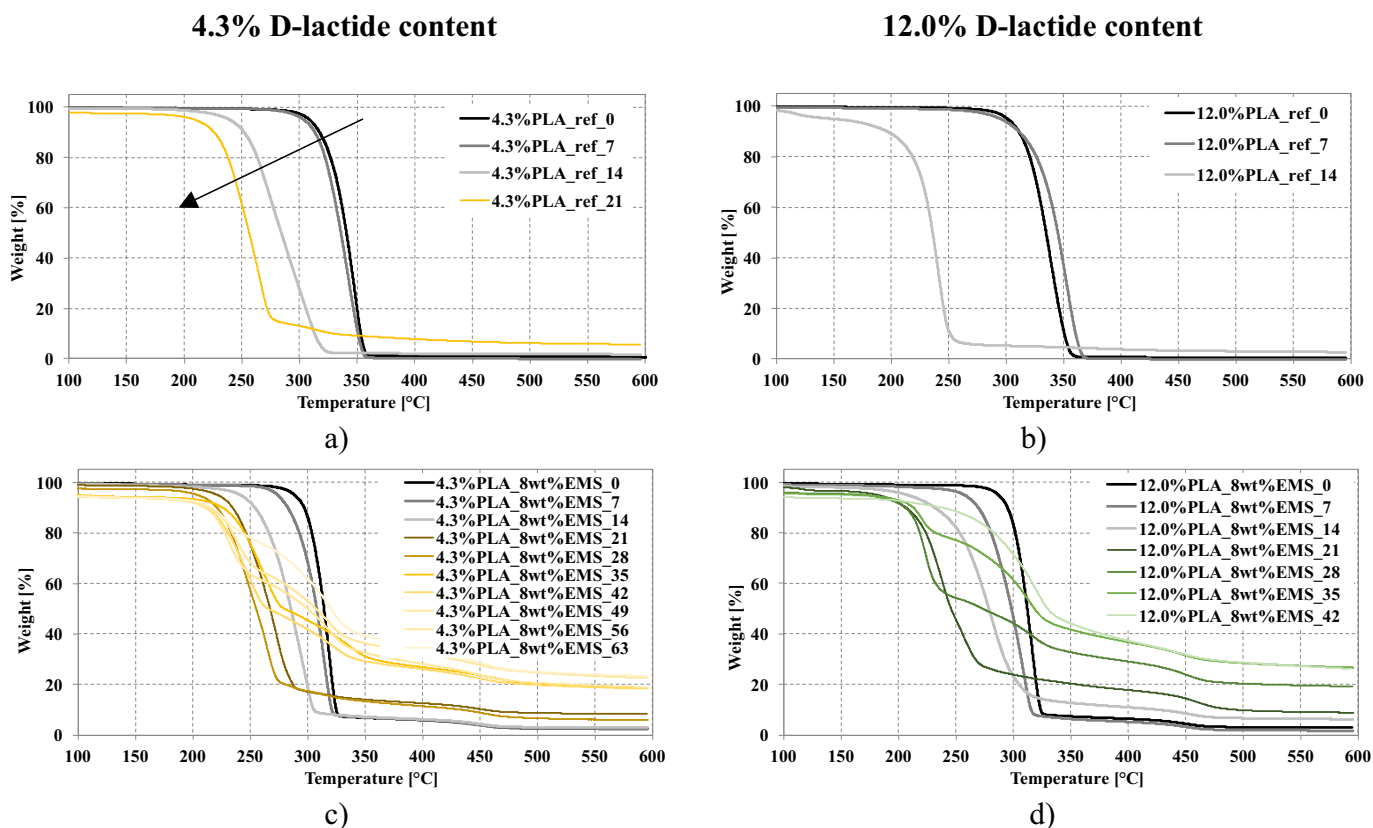


Fig. 4. TGA curves of composted foams as a function of temperature a) 4.3%PLA\_ref, b) 12.0%PLA\_ref, c) 4.3%PLA\_8wt%EMS, d) 12.0%PLA\_8wt%EMS.

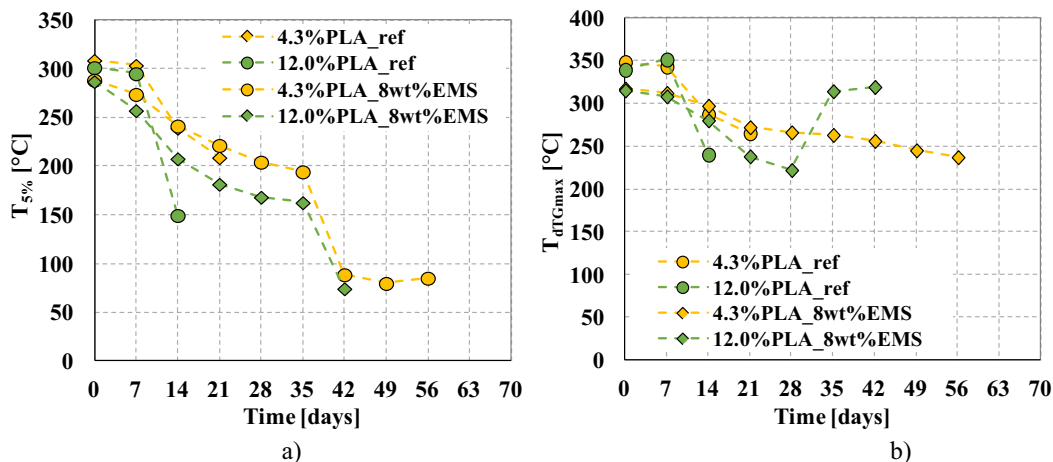


Fig. 5. TGA results of PLA samples a)  $T_{5\%}$ , b)  $T_{dTGmax}$  as a function of composting time.

Table 1

The crystalline fraction of PLA samples with 4.3% D-lactide content calculated from DSC results as a function of composting time.

Composting time (days)	Crystalline fraction from 2nd heat up [%]									
	0	7	14	21	28	35	42	49	56	63
4.3%PLA_ref	28.5	35.2	44.0	31.3	-	-	-	-	-	-
12.0%PLA_ref	0.0	0.0	0.0	-	-	-	-	-	-	-
4.3%PLA_8wt%EMS	29.3	33.7	40.0	34.1	20.1	6.9	1.8	0.0	0.8	-
12.0%PLA_8wt%EMS	0.0	0.0	0.0	0.0	0.0	0.0	0.0	-	-	-

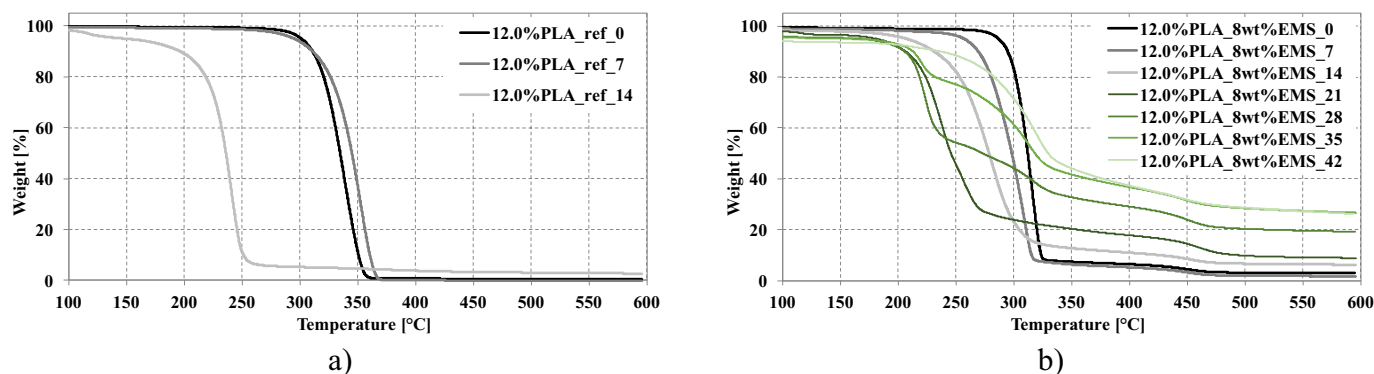


Fig. 6. TGA curves of composted foams as a function of temperature a) 12.0%PLA\_ref, b) 12.0%PLA\_8wt%EMS.

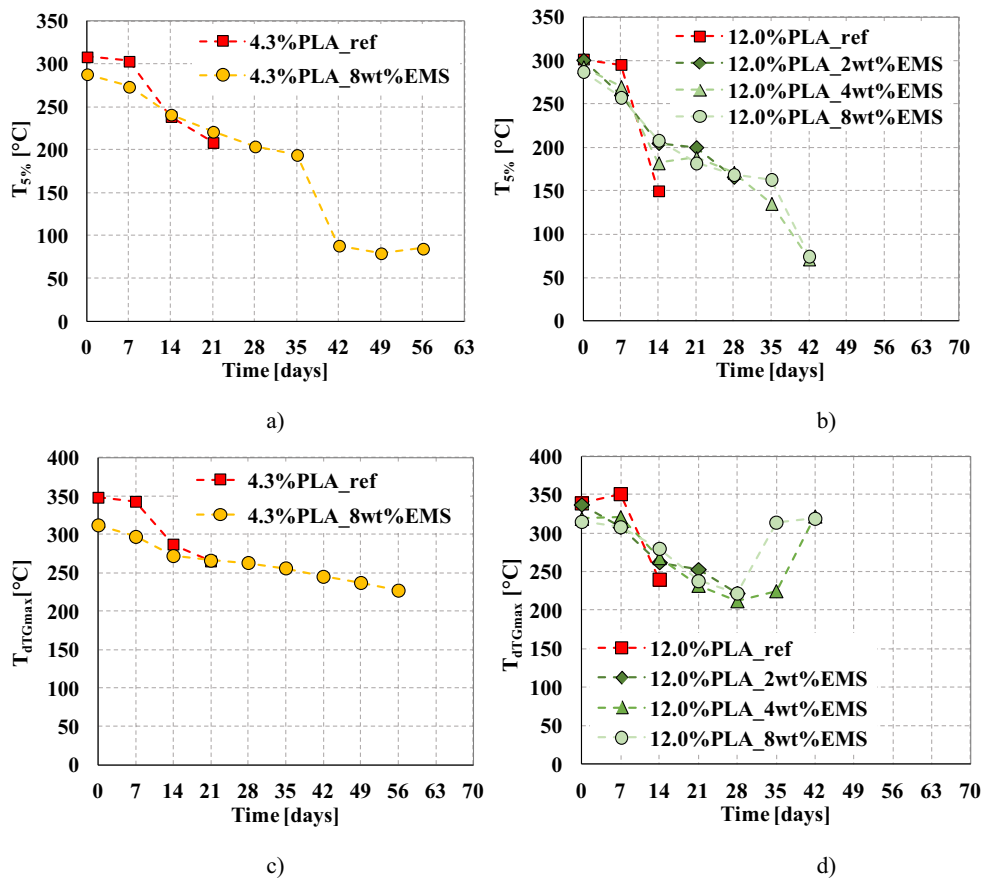


Fig. 7. TGA results of PLA samples a) and b)  $T_{5\%}$ , c) and d)  $T_{dT_{Gmax}}$  as a function of composting time.

%EMS was 25.2 J/g. After 7 days of composting, the PLA with 4.3% D-lactide content crystallized; therefore  $\Delta H_{cc}$  decreased to 0 J/g both in the case of the 4.3%PLA\_ref sample and 4.3%PLA\_8wt%EMS. The increased crystalline fraction after 7 days of composting causes a difference in the number of days required for disintegration, because the degradation time is shorter for amorphous PLA due to the water diffusion through amorphous PLA [44].

The crystalline fraction of the samples from the second heating cycle was also evaluated (Table 1). From day 0 until day 21, the percentage of the crystalline fraction did not change much and was around 30%. While the 4.3% PLA\_ref sample was already decomposed on day 28, the foam sheet sample containing 8 wt% EMS was only decomposed on day 63. In the case of the 4.3% PLA\_8wt% EMS foam sheet, a slow decrease of the crystalline fraction was observed after day 21. This is due to chain

scission caused by hydrolytic degradation. As a result of chain scission, the polymer chains become shorter, therefore the crystals they can form are imperfect. Due to the shorter chains, the number of chain ends increases, the chain ends are not able to participate in the arrangement and folding of the chains, thus inhibiting the formation of large and complete crystals. Furthermore, as degradation progressed, the resulting monomers and oligomers also decreased the crystallinity of PLA [47].

### 3.2. The effect of thermally expandable microsphere content on the compostability of poly(lactic acid)-based foam structures

The number of days required for degradation is given in Fig. 1. Based on the results the decomposition time increases with increasing thermally expandable microsphere content. The decomposition process was

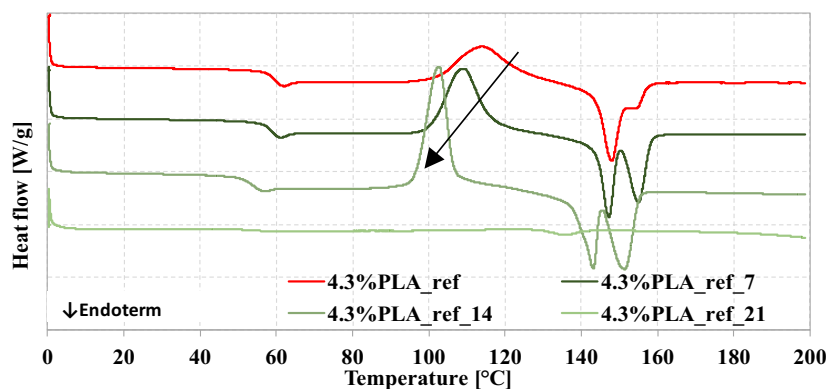


Fig. 8. DSC curves of composted foams as a function of temperature 4.3%PLA\_ref.

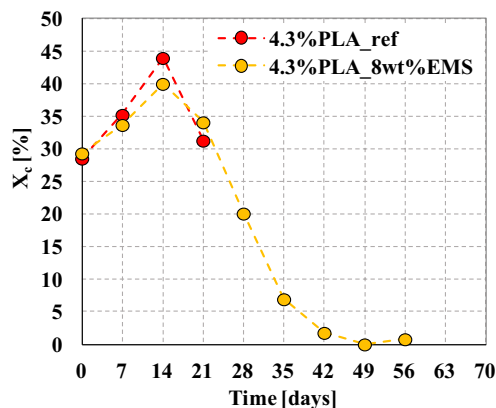


Fig. 9. a) and b) crystalline fraction of PLA samples calculated from DSC (2nd heating) of PLA samples as a function of composting time.

followed using TGA (Fig. 6) and the initial decomposition value ( $T_{5\%}$ ) determined from the TGA shows a decreasing trend as a function of composting time until the moment before complete decomposition (Fig. 7 a and b). The rate of decrease is highest for the unfoamed reference PLA sheets. At  $T_{dT_{Gmax}}$  (Fig. 7 c and d, Supplementary A.7) and at  $T_{50\%}$  (Supplementary A.8), the rate of decrease is also highest for the reference PLA sheets. If the PLA also contains thermally expandable microspheres, the decrease in  $T_{dT_{Gmax}}$  is less. Furthermore, there is a point where both values start to increase. This is because during degradation, as the PLA content decreases, the shell material of the foaming agent, methyl methacrylate (MMA), starts to dominate at  $T_{dT_{Gmax}}$ .

PLA with 4.3% D-lactide content (4.3%PLA\_ref) cold crystallized during the DSC test (Fig. 8 and Supplementary A.9 a) on day 0. From day 21,  $\Delta H_{cc}$  became 0 J/g because the samples with 4.3% D-lactide content formed a crystalline fraction during the first composting week. The PLA reference sample with 12.0% D-lactide content, did not crystallize either during the DSC test or during composting. Foamed PLA samples containing 12.0% D-lactide also remained amorphous (Supplementary A.9 b). Until day 21, the crystalline fraction of both non-foamed and foamed sheet samples produced with PLA containing 4.3% D-lactide increased (Fig. 9). After 21 days, the 4.3%PLA\_ref sample decomposed. In the case of the 4.3%PLA foamed with 8 wt% EMS, the decrease in  $\chi_c$  was a long and steep process. The crystalline fraction of 4,3%PLA\_8wt%EMS reached 0% on day 49 and decomposition took place on day 63. In polylactic acid-based foams, the thermally expandable microspheres cause a decrease in the rate of degradation. Diffusion in polymers is commonly described by the Fickian diffusion model, although syntactic foam above 40 °C cannot be modeled by Fick's law [48]. Therefore not

only matrix hydration takes place, but other mechanisms, such as the hydration of the expandable microsphere and polymer matrix interface as well [48].

In summary, in a poly(lactic acid)-based system, a thermally expandable microsphere-type foaming agent causes a decrease in the rate of degradability. This is because the syntactic foam structure is less permeable to moisture and microorganisms [28,49].

#### 4. Conclusions

We investigated the compostability of foam structures produced with an EMS foaming agent from poly(lactic acid)s of different D-lactide contents, and also. Examined the effect of foaming agent content on the degradability of biopolymer-based foam structures. The results suggest that PLA with higher D-lactide content has a faster degradation process, as the rate of hydrolysis depends on the basic properties of PLA, such as its crystallinity and initial molecular weight. This is because, during composting, the polymer chains are broken by hydrolytic degradation, and the length of the polymer chains is reduced. Shorter polymer chains are degraded at lower temperatures. The effect of EMS on the compostability of extruded PLA foam sheets was examined and the results indicated that the foaming agent caused a decrease in the rate of degradation. Still, the smallest, medium-density foams ( $0.401 \pm 0.007$  g/cm<sup>3</sup>) also degraded before day 70. Thanks to the latest developments, microspheres that are bio-based [50] and preferably biodegradable will be available. In this way, the results can be applied to such new types of environmentally friendly foaming agents.

#### Funding

The research reported in this paper and carried out at BME has been supported by the NRD Fund (TKP2020 IES, Grant No. BME-IE-NAT; TKP2020 NC, Grant No. BME-NC) based on the charter of bolster issued by the NRD Office under the auspices of the Ministry for Innovation and Technology. This paper was supported by the National Research, Development and Innovation Office (K 132462). The research reported in this paper was supported by H2020-MSCA RISE No. 872152 - GREEN-MAP project of the European Union. Prepared with the professional support of the Doctoral Student Scholarship Program of the Co-operative Doctoral Program of the Ministry for Innovation and Technology from the source of the National Research, Development and Innovation Fund (D. Gere). Á. Kmetty is thankful for the support of ÚNKP-21-5 New National Excellence Program of the Ministry for Innovation and Technology from the source of the National Research, Development and Innovation Fund. Á. Kmetty also thanks to the support of János Bolyai Research Scholarship of the Hungarian Academy of Sciences.

Data availability

The raw/processed data required to reproduce these findings cannot

be shared at this time as the data also forms part of an ongoing study.

### CRedit authorship contribution statement

**Katalin Litauszki:** Methodology, Investigation, Validation, Formal analysis, Writing – original draft, Visualization. **Daniel Gere:** Methodology, Investigation, Validation, Formal analysis, Visualization, Writing – original draft. **Tibor Czigan:** Conceptualization, Supervision. **Ákos Kmetty:** Conceptualization, Supervision, Writing – review & editing, Project administration.

### Declaration of Competing Interest

The authors declare that they have no known competing financial interests or personal relationships that could have appeared to influence the work reported in this paper.

### Data availability

The authors do not have permission to share data.

### Acknowledgments

We would like to thank Tramaco GmbH (Germany) and to INTERDIST Kft. (Hungary) for the Tracel G 6800 MS foaming agent.

### Appendix A. Supplementary data

Supplementary data to this article can be found online at <https://doi.org/10.1016/j.susmat.2022.e00527>.

### References

- [1] Association of Plastics Manufacturers, *Plastics – The Facts 2021: An Analysis of European Plastics Production, Demand and Waste Data*, 2021. Belgium.
- [2] A.L. Patricio Silva, et al., Rethinking and optimising plastic waste management under COVID-19 pandemic: policy solutions based on redesign and reduction of single-use plastics and personal protective equipment, *Sci. Total Environ.* 742 (2020), 140565.
- [3] T. Czigan, F. Ronkay, Plastics in the shadow of the coronavirus: Don't prohibit, teach instead!, *Express Polym Lett* 15 (6) (2021) 490–491.
- [4] R. Ajwani-Ramchandani, et al., Enhancing the circular and modified linear economy: the importance of blockchain for developing economies, *Resour. Conserv. Recycl.* (2021) 168.
- [5] W. Queiroz de Oliveira, et al., Food packaging wastes amid the COVID-19 pandemic: trends and challenges, *Trends Food Sci. Technol.* 116 (2021) 1195–1199.
- [6] F. Ronkay, et al., Plastic waste from marine environment: demonstration of possible routes for recycling by different manufacturing technologies, *Waste Manag.* 119 (2021) 101–110.
- [7] R. Panchal, A. Singh, H. Diwan, Does circular economy performance lead to sustainable development? – a systematic literature review, *J. Environ. Manag.* 293 (2021).
- [8] K. Navare, et al., Circular economy monitoring – how to make it apt for biological cycles? *Resour. Conserv. Recycl.* (2021) 170.
- [9] G. Fredi, A. Dorigato, Recycling of bioplastic waste: a review, *Adv. Indus. Eng. Polym. Res.* 4 (2021) 133–222.
- [10] H. Lu, et al., Toward Strong and Super-Toughened PLA Via Incorporating a Novel Fully Bio-Based Copolyester Containing Cyclic Sugar. *Composites Part B: Engineering*, 2021, p. 207.
- [11] European Bioplastics, *Frequently Asked Questions on Bioplastics*, European Bioplastics e.V, Berlin, 2021.
- [12] S. Ahmed, S. Kanchi, G. Kumar, *Handbook of Biopolymers: Advances and Multifaceted Applications*, Pan Stanford Publishing Pte. Ltd., Singapore, 2019.
- [13] European Bioplastics, *What Are Bioplastics?*, Available from: [www.european-bioplastics.org](http://www.european-bioplastics.org), 2022.
- [14] K.E. Mazur, et al., Mechanical, thermal and hydrodegradation behavior of poly (3-hydroxybutyrate-co-3-hydroxyvalerate) (PHBV) composites with agricultural fibers as reinforcing fillers, *Sustain. Mater. Technol.* (2022) 31.
- [15] L. Dilkes-Hoffman, et al., Public attitudes towards bioplastics – knowledge, perception and end-of-life management, *Resour. Conserv. Recycl.* (2019) 151.
- [16] D. Gere, T. Czigan, Future trends of plastic bottle recycling: Compatibilization of PET and PLA, *Polym. Test.* 81 (2019), 106160.
- [17] M.M. Hanon, R. Marczis, L. Zsidai, Influence of the 3D printing process settings on tensile strength of PLA and HT-PLA, *Period. Polytech. Mech. Eng.* 65 (1) (2020) 38–46.
- [18] J. Yun-Wan, et al., Synergy Effect between Quaternary Phosphonium Ionic Liquid and Ammonium Polyphosphate toward Flame Retardant PLA with Improved Toughness. *Composites Part B: Engineering*, 2020, p. 197.
- [19] M.L. Di Lorenzo, R. Androsch, *Industrial Applications of Poly(lactic acid)*, Springer Nature, Cham, Switzerland, 2018.
- [20] Weiwei Cui, et al., CO<sub>2</sub>-assisted fabrication of PLA foams with exceptional compressive property and heat resistance via introducing well-dispersed stereocomplex crystallites *Journal of CO<sub>2</sub> utilization, J. CO<sub>2</sub> Utiliz.* 64 (2022), 102184.
- [21] Xinyi Wei, et al., ScCO<sub>2</sub>-assisted fabrication and compressive property of poly (lactic acid) foam reinforced by in-situ polytetrafluoroethylene fibrils, *Int. J. Biol. Macromol.* 209 (2022) 2050–2060.
- [22] IFBB – Institute for Bioplastics and Biocomposites, *Biopolymers - Facts and Statistics* 2020, 2020.
- [23] M. Karamanlioglu, R. Preziosi, G.D. Robson, Abiotic and biotic environmental degradation of the bioplastic polymer poly(lactic acid): a review, *Polym. Degrad. Stab.* 137 (2017) 122–130.
- [24] Biodegradable polymers and polymer blends, in: L. Jiang, J. Zhang, S. Ebnesajjad (Eds.), *Handbook of Biopolymers and Biodegradable Plastics*, William Andrew Publishing, Boston, MD, USA, 2013.
- [25] M. Karamanlioglu, G.D. Robson, The influences of biotic and abiotic factors on the rate of degradation of poly (lactic acid) (PLA) coupons buried in compost and soil poly (lactic acid) (PLA) coupons buried in compost and soil, *Polym. Degrad. Stab.* 98 (10) (2016) 2063–2071.
- [26] L. Avérous, *Handbook of Biopolymers and Biodegradable Plastics*, Plastics Design Library, Plastics Design Library, Oxford, 2013.
- [27] G. Gorrasi, R. Pantani, Effect of PLA grades and morphologies on hydrolytic degradation at composting temperature: assessment of structural modification and kinetic parameters, *Polym. Degrad. Stab.* 98 (2013) 1006–1014.
- [28] J. Sarasa, et al., Study of the biodegradation of a bioplastic material waste, *Bioresour. Technol.* 100 (2009) 3764–3768.
- [29] G.V.M. Zimmermann, et al., Observations of the effects of different chemical blowing agents on the degradation of poly(lactic acid) foams in simulated soil, *Mater. Res.* 16 (6) (2013) 1266–1273.
- [30] T. Standau, et al., Chemical modification and foam processing of Polylactide (PLA), *Polymers* 11 (2019) 306.
- [31] K. Litauszki, Á. Kmetty, Extrusion foaming of poly(lactic acid) with thermally expandable microspheres. *SPE Foams*, 2019. Valladolid, Spain.
- [32] C. Huang, N.L. Thomas, Fabricating porous poly(lactic acid) fibres via electrospinning, *Eur. Polym. J.* 99 (2018) 464–476.
- [33] G. Wang, et al., Strong and super thermally insulating in-situ nanofibrillar PLA/PET composite foam fabricated by high-pressure microcellular injection molding, *Chem. Eng. J.* 390 (2020), 124520.
- [34] K. Bocz, et al., Optimal distribution of phosphorus compounds in multi-layered natural fabric reinforced biocomposites, *Express Polym Lett* 14 (2020) 606.
- [35] T. Li, et al., High-performance poly(lactic acid) composites reinforced by artificially cultured diatom frustules, *Mater. Des.* 195 (2020), 109003.
- [36] E. Castro-Aguirre, et al., Poly(lactic acid) - mass production, processing, industrial Applications, and end of life, *Adv. Drug Deliv. Rev.* 107 (2016) 333–366.
- [37] R. Auras, et al., *Poly(Lactic Acid) Synthesis, Structures, Properties, Processing and Applications*, Wiley, New Jersey, 2011.
- [38] X. Xu, et al., Effects of die geometry on cell nucleation of PS foams blown with CO<sub>2</sub>, *Polym. Eng. Sci.* 43 (2003) 1378–1390.
- [39] ISO 20200:2015, *Plastics — determination of the degree of disintegration of plastic materials under simulated composting conditions in a laboratory-scale test*, 2015.
- [40] T. Tábi, S. Hajba, J.G. Kovács, Effect of crystalline forms ( $\alpha'$  and  $\alpha$ ) of poly(lactic acid) on its mechanical, thermo-mechanical, heat deflection temperature and creep properties, *Eur. Polym. J.* 82 (2016) 232–243.
- [41] T. Tábi, T. Ageyeva, J.G. Kovács, The influence of nucleating agents, plasticizers, and molding conditions on the properties of injection molded PLA products, *Mater. Today Commun.* (2022) 32.
- [42] M. Mohammadi, et al., Interfacial localization of CNCs in PLA/PBAT blends and its effect on rheological, thermal, and mechanical properties, *Polymer* 233 (2021).
- [43] M.P. Arrieta, et al., Disintegrability under composting conditions of plasticized PLA-PHB blends, *Polym. Degrad. Stab.* 108 (2014) 307–318.
- [44] T. Maharana, B. Mohanty, Y.S. Negi, Melt–solid polycondensation of lactic acid and its biodegradability, *Prog. Polym. Sci.* 34 (1) (2009) 99–124.
- [45] M. Karimi-Avargani, et al., The promiscuous potential of cellulase in degradation of poly(lactic acid) and its jute composite, *Chemosphere* 278 (2021), 130443.
- [46] E. Castro-Aguirre, et al., Insights on the aerobic biodegradation of polymers by analysis of evolved carbon dioxide in simulated composting conditions, *Polym. Degrad. Stab.* 137 (2017) 251–271.
- [47] Y. Zare, R. Kyong Yop, Following the morphological and thermal properties of PLA/PEO blends containing carbon nanotubes (CNTs) during hydrolytic degradation, *Compos. Part B* (2019) 175.
- [48] X. Lefebvre, et al., Durability of syntactic foams for deep offshore insulation: modelling of water uptake under representative ageing conditions in order to predict the evolution of buoyancy and thermal conductivity, *Oil Gas Sci. Technol.* 64 (2) (2009) 165–178.
- [49] N. Gupta, et al., Foam testing, in: Chun-Hway Hsueh (Ed.), *Handbook of Mechanics of Materials*, Springer, Singapore, 2019.
- [50] J. Sameni, et al., Preparation and characterization of biobased microspheres from lignin sources, *Ind. Crop. Prod.* 117 (2018) 58–65.